communications earth & environment

Article

https://doi.org/10.1038/s43247-024-01657-4

Moderate and high-temperature metamorphic conditions produced diverse phosphorous species for the origin of life

Check for updates

Abu Saeed Baidya [1] ✉, Matthew Adam Pasek [2] & Eva E. Stüeken [1]

Low solubility and low reactivity towards organic compounds make phosphorus a problematic element for the origin and early evolution of life. Reduced and polymerized phosphorus species are more bioavailable and may resolve these issues, but widespread formation pathways for these species are not well understood. Here we show, using experiments and thermodynamic modelling, that diverse polyphosphates (straight-chains with up to five and cyclophosphates with three and four phosphate molecules) and reduced phosphite can form under ferruginous anhydrous conditions at 80-700 °C. We find that hydrogen and temperature enhance phosphite production while polyphosphate formation maximizes at moderate temperatures (175-200 °C). Chromite and Nickel-bearing minerals enhance phosphate polymerization and reduction whereas magnetite inhibits them. These findings expand on previous investigations of thermally induced changes in phosphorus-speciation and show that these reactions may be widespread in nature. Metamorphism of ferruginous sediments, serpentinization, as well as subaerial lakes exposed to volcanic heating could potentially produce a wealth of polyphosphates along with phosphite on the early Earth. Later, these species may have participated in prebiotic phosphorylation reactions upon liberation by subsequent fluid infiltration. Our results thus offer a more widespread pathway for the generation of reactive phosphorus for the origin of life.

Phosphorus-bearing organic compounds are essential for cellular structure (phospholipids), metabolic energy transfer (ATP), and information storage (DNA, RNA) in all known forms of life. However, phosphorus is less abundant than other bioessential major elements (C, H, O, N, S)[1] and is mostly locked in sparsely-soluble phosphate (P(V)) minerals (e.g., hydroxylapatite ($Ca_{10}(PO_4)_6(OH)_2$))[2]. Phosphorus is therefore a limiting nutrient for marine bioproductivity across geologic timescales[3] and may have hindered the prebiotic formation of phosphorylated organic compounds that are necessary for the origin of life[4–6]. Low solubility of phosphate in water and its low reactivity toward the organic compounds (i.e. phosphorylation) are collectively known as "Phosphate Problem" for the origin of life.

Several hypotheses have been developed to resolve the solubility issue with phosphate including its presence in carbonate-rich alkaline lakes[7], or in urea-ammonium formate-rich solutions with low water activity that enhance the solubility of natural phosphate mineral including apatite[8]. It has also been proposed that the early ocean contained higher levels of dissolved phosphate than previously thought due to new constraints on the solubility of vivianite[9]. However, these hypotheses have several limitations. For example, in alkaline lakes concentrations of metal micronutrients such as Fe, Cu, and Zn required for the origin and survival of life are limited, and natural environments with millimolar level urea and ammonium formate have yet to be discovered. Similarly, for the open ocean, changes in pH and Ca concentration or conditions that favor greenalite or ferrihydrite precipitation may have reduced phosphate availability below experimental predictions.

An alternative solution to the low solubility of phosphate (Pi) may be the conversion to reduced P such as phosphite (HPO_3^{2-}, P(III)) that is ca. 1,000 times more soluble than phosphate in natural fluids including seawater in the presence of bivalent metals such as Ca, Mg, and Fe(II)[2,10,11]. Phosphite has been detected in Archean metasedimentary rocks[12] and has

[1]School of Earth & Environmental Sciences, University of St Andrews, St Andrews, Fife, KY16 9TS, UK. [2]School of Geosciences, University of South Florida, Tampa, FL, 33620, USA. ✉e-mail: asb27@st-andrews.ac.uk

been utilized by life since at least the Neoarchean-Paleoproterozoic[13]. Phosphite has also been shown to be more efficient than phosphate in the formation of organophosphorus compounds (phosphonylation vs. phosphorylation)[14].

Phosphorylation, the second aspect of the "phosphate problem", is key to the origin of life as phosphorylated compounds, in particular nucleotides, are a prerequisite for the RNA-world[15]. Two major abiotic pathways are known to make them. The first pathway involves the formation of nucleosides from ribose and nucleobases followed by phosphorylation of nucleosides[16–19]. In the second pathway, ribose phosphate is formed from ribose and a phosphate precursor (dissolved phosphate or apatite), followed by addition of a nucleobase[20,21]. Although the latter mimics modern biology and is possible in the presence of low dissolved phosphate concentrations, these pathways require borate to stabilize ribose and execute the reactions. The availability of borate may have been restricted to certain parts of the prebiotic Earth as evident from rare reports of elevated boron levels in Archean sedimentary rocks[22]. In the absence of borate, the first pathway of nucleotide formation is more likely; in that case, polyphosphates would be better phosphorylating agents than orthophosphate as they are more reactive towards organic matter[6,14,23].

Polyphosphates are also known as condensed phosphates that include long-chain polyphosphate such as pyrophosphate (PP_i), triphosphate (PPP_i), tetra- and other higher-order phosphates ($PPPP_i$+), and cyclophosphates such as trimetaphosphate (PPPc) and tetrametaphosphate (PPPPc). Polyphosphates are also considered a possible predecessor of ATP, i.e. the energy currency of all life on Earth[24]. Cyclophosphates in particular may act both as polymerizing and phosphorylating agents, e.g., they can be precursors of amidophosphate and are capable of phosphorylating glyceric acid, sugars, amino acids, and nucleosides[6,23,25]. Furthermore, PPPc may react with ammonium to produce diamidophosphate[26], which can react with diols, forming cyclic phosphates including ribose 1-,2-cyclic phosphate, a phosphorylated compound that can form canonical ribonucleotides with the direct reaction to nucleobases[27,28]. Given the importance of phosphite and the polyphosphates, it is imperative to determine if and where these alternative P species could have been produced in significant abundances on the early Earth[29].

Three main mechanisms have been proposed for phosphite formation on the prebiotic Earth including (1) water-induced oxidation of schreibersite (i.e. $(Fe,Ni)_3P$)[30,31], which was either delivered by meteorites[32] or produced in lightning-struck soil[33]; (2) reduction of apatite during lightning in volcanic ash clouds[34]; and (3) reduction of phosphate coupled to Fe^{2+} oxidation under anhydrous conditions at elevated temperature (180 °C)[11]. Among these mechanisms, Fe^{2+}-induced phosphate reduction has the potential to be the most widespread. A natural example of this mechanism includes the diagenesis of ferruginous sediments[11] and serpentinization of ultramafic rocks containing olivine[35]. There is, however, only one experiment that explored Fe(II)-induced phosphate reduction so far, and it was limited to 180 °C. Little is known about the yields of phosphite formation by Fe(II)-induced reduction under a wide range of geologic conditions relevant to prebiotic Earth, and the role of other reducing agents such as H_2 and mineral catalysts, particularly Fe-, Ni-, and Cr-bearing minerals, are unknown.

The formation of polyphosphates, on the other hand, has been demonstrated (1) from pure phosphates (e.g., $NaH_2PO_4/NH_4H_2PO_4$) at 80–1200 °C[36,37]; (2) in high-temperature (>1200 °C) volcanic systems[38]; and (3) via metallic phosphide dissolution at ambient temperatures[39]. However, these scenarios would likely have been rare on early Earth and Mars. For example, the pure sodium or ammonium phosphate salt systems may not exist in nature, and temperatures above 1200 °C where they might exist are relatively rare[5]. More widespread near the surface would have been ferruginous sedimentary environments that underwent thermal effects (diagenesis and metamorphism), similar to those found to yield reduced P[11,35]. One study conducted at 180 °C under ferruginous conditions demonstrated PPi formation with a yield of 15%[11]. Hence metamorphic sedimentary settings may be conducive to P polymerization in addition to reduction and may have provided the reactive P species required for the origin of life. However, the formation of higher-order polyphosphates in such settings has so far not been demonstrated, and it is unknown how polymerization yields vary as a function of temperature. Furthermore, it has been proposed that amorphous silica may facilitate polymerization in alkali phosphate systems[40,41]; however, the effects of other prebiotically relevant minerals on phosphate polymerization in ferruginous environments has not yet been explored.

Here we address this knowledge gap about phosphite and polyphosphate formation in ferruginous settings on early Earth by greatly expanding on the parameter space explored previously[11]. To mimic these settings, we carried out thermodynamic modeling and experiments and measured P speciation between 85 and 700 °C in acidic ferruginous conditions and in the presence of different mineral substrates and N_2 and/or H_2 gas (see Supplementary Fig. S1 for the experimental set-ups). We prepared solutions of sodium phosphate and iron(II) chloride (Fe:P = 3:1 molar ratio) and let these evaporate to dryness at 60 °C under vacuum or constant flow of N_2 gas, followed by pulverizing and further heating at 170–700 °C under static N_2 or H_2 or under a flow-through N_2 or H_2 (5%) atmosphere for up to one week, maintaining an anoxic environment throughout. Magnetite, chromite, pyrite, Ni, Fe, and Ni-sulfide were added to the solution before evaporation (see "Methods" for details). In two static experiments, the gas phase was briefly vented after 3 h and 24 h, respectively, to further enhance water removal. The final solids were analysed by XRD. Phosphorus species were extracted with EDTA-NaOH solutions and analysed by NMR and IC-ICPMS. Our data shed new light on the speciation of phosphorus on the early Earth.

Results

Mineralogy of evaporated and heated residues

The experimental conditions and the major results are summarized in Tables 1, 2, respectively. In general, the evaporated solid was composed of halite (NaCl), rokuenite ($FeCl_2{\cdot}2H_2O$), and an amorphous Fe-PO_4 phase, irrespective of evaporation method (vacuum or N_2 flow-through) (Fig. 1, Table 2). Crystalline vivianite ($Fe_3(PO_4)_2{\cdot}8H_2O$) is the most stable phase in the Fe-PO_4 system, whose crystallization takes place through an intermediate water-poor amorphous phase ($Fe_3(PO_4)_2{\cdot}4.7H_2O$)[42]. In our case, vivianite was not observed, but we detected an amorphous Fe(II)-phosphate phase. We tentatively identify this phase as $Fe_3(PO_4)_2{\cdot}xH_2O$ where x is between 0 to ≤8. The mineralogy of the Fe-/Ni-/Cr-bearing phases remained the same, and they did not affect the composition of the evaporated residues.

The mineralogy of the heated residues at 200 °C under static N_2 or H_2 was broadly similar to that of the evaporation stage (Fig. 1). In contrast, the N_2 flow-through experiments at 170 and 200 °C contained anhydrous $FeCl_2$ instead of rokuenite (Fig. 1). The 350 °C heated residues from static N_2/H_2 and N_2 flow-through experiments lacked amorphous phases and were instead dominated by Fe-hydroxide ($Fe(OH)_2$,), Fe-chlorides ($FeCl_2$ and $FeCl_2{\cdot}2H_2O$), Fe-phosphates (possibly $NaFePO_4$ and an unidentified Fe-PO_4 phase), NaCl, and other unidentified phases (Fig. 1). The added Fe-/Ni-/Cr-bearing phases remained mostly unchanged. In H_2-flow experiments, Fe, NaCl, and Fe-phosphates (most likely $NaFePO_4$ i.e. maricite and an unidentified Fe-PO_4 phase), and other identified phases were produced at 600 °C, while Fe and $Fe_3(PO_4)_2$ are observed at 700 °C (Supplementary Fig. S2).

P speciation in solution

After the evaporation step, most P remained in the form of phosphate. Less than 2% PPi was generated, and no other polyphosphates or phosphite were detected (detection limits are 0.05% and 0.001% of initial P, respectively). In contrast, further heating yielded variable proportions of polymerized P and small but detectable amounts of reduced P species (Fig. 2, Table 2).

Phosphate polymerization and speciation were found to be highly dependent on temperature. The highest yield of polymerization (70%) and the largest number of polymerized P species were detected at 170 °C with 19% PPi, 24% PPPi, and 26% PPPPi+ (Figs. 2, 3A, B). This is the only

Table 1 | Summary of the experiments

T [°C]	Exp. No.	Starting composition	Drying method	Pre-heating	Heating stage
Evaporation Exp.					
85	E1	A - $FeCl_2.4H_2O$:NaH_2PO_4 = 3:1, pH 4	N_2 flow	-	-
60	E2	A - $FeCl_2.4H_2O$:NaH_2PO_4 = 3:1, pH 4[#]	vacuum	-	-
Static atmosphere:					
200	S1 A S1 B	A. $FeCl_2.4H_2O$:NaH_2PO_4 = 3:1, pH 1–2	vacuum, 50 °C	None	A. 4 days, N_2 B. 7 days, N2
		B. FeCl2.4H2O:NaH2PO4 = 3:1, pH 4[#]			
200	S2 A S2 B	A - $FeCl_2.4H_2O$:NaH_2PO_4 = 3:1, pH 1–2	vacuum, 50 °C	200 °C, 24 hours, N_2 flushing	7 days, H_2
		B - $FeCl_2.4H_2O$:NaH_2PO_4 = 1:1, pH 1–2			
200	S3 A-G	A - $FeCl_2.4H_2O$:NaH_2PO_4 = 3:1, pH 4	vacuum, 50 °C	200 °C, 3-24 hours, N_2 flushing	7 days, H_2
		B* - $FeCl_2.4H_2O$:NaH_2PO_4:magnetite = 3:1:0.5, pH 4			
		C - $FeCl_2.4H_2O$:NaH_2PO_4:pyrite = 3:1:1, pH 4			
		D - $FeCl_2.4H_2O$:NaH_2PO_4:Ni:Fe = 3:1:0.75:0.25, pH 4			
		E* - $FeCl_2.4H_2O$:NaH_2PO_4:Ni = 3:1:1, pH 4			
		F - $FeCl_2.4H_2O$:NaH_2PO_4:Ni_3S_2 (heazlewoodite) = 3:1:0.5, pH 4			
		G - $FeCl_2.4H_2O$:NaH_2PO_4:chromite = 3:1:0.5, pH 4			
350	S4	$FeCl_2.4H_2O$:NaH_2PO_4 = 3:1, pH 4	vacuum, 50 °C	None	7 days, N_2
350	S5A-E	A - $FeCl_2.4H_2O$:NaH_2PO_4:magnetite = 3:1:0.5, pH 4	vacuum, 50 °C	None	7 days, H_2
		B - $FeCl_2.4H_2O$:NaH_2PO_4:Ni_3S_2 (heazlewoodite) = 3:1:0.5, pH 4			
		C - $FeCl_2.4H_2O$:NaH_2PO_4:Ni:Fe = 3:1:0.75:0.25, pH 4			
		D - $FeCl_2.4H_2O$:NaH_2PO_4:chromite = 3:1:0.5, pH 4			
		E - $FeCl_2.4H_2O$:NaH_2PO_4:Ni = 3:1:1, pH 4			
Flow-through:					
170	F1	A - $FeCl_2.4H_2O$:NaH_2PO_4 = 3:1, pH 4[#]	N_2 flow, 60 °C	None	7 days, N_2
200	F2 A F2 B	A* - $FeCl_2.4H_2O$:NaH_2PO_4 = 3:1, pH 4[#]	vacuum, 50 °C & N_2 flow, 60 °C	None	7 days, N_2
		B* - $FeCl_2.4H_2O$:NaH_2PO_4:olivine = 3:1:1, pH 4			
350	F3	$FeCl_2.4H_2O$:NaH_2PO_4 = 3:1, pH 4[#]	N_2 flow, 60 °C	None	7 days, N_2
600	F4	$FeCl_2.4H_2O$:NaH2PO4 = 3:1, pH 4[#]	N_2 flow, 60 °C	None	10 hours, 95% N_2 + 5% H_2
700	F5	$FeCl_2.4H_2O$:$NH_4H_2PO_4$ = 3:1, pH 4[#]	vacuum, 60 °C	None	2 hours, 95% N_2 + 5% H_2

[#] pH measured after adding the salt; [*]replicated 2–4 times.

experiment where penta- and possibly hexapolyphosphate were formed (Fig. 2). A second analysis of this solution, after 50 days of storage at room temperature, showed near identical total yields (70%); however, the speciation had changed to 61% PPi, 5% PPPi, 4% PPPc, and most likely 0.3% PPPPc[38] (Figs. 2, 3B). Polymerization yields and diversity decreased in experiments above 170 °C (Figs. 2, 3A). For example, at 200 °C, the average yield was 44% with 38% PPi, 5% PPPi, and 1% PPPPi+ while at 350 °C, the yield decreased to only 0.2% PPi. Polymerization was undetectable at 600 °C and 700 °C (Figs. 2, 3C).

Polymerization yields were higher when water could escape more efficiently during heating. N_2 flow-through experiments where water vapor was constantly flushed out showed higher yields compared to static N_2 experiments (e.g., at 200 °C, yields were 44% and 15% under flow-through and static conditions, respectively). Similarly, the 200 °C static H_2 experiment, where the gas was vented briefly after 24 h, shows a higher polymerization yield (56% with 44% PPi, 9% PPPi, and 1% PPPPi +) compared to when venting occurred after 3 h (total 19.3% with 19% PPi and 0.3% PPPi).

Mineral substrates impacted the polymerization yield. The presence of chromite and Fe/Ni or their sulfides increased yields up to 10 times at 200 °C, while magnetite supressed polymerization (Fig. 3C; Supplementary Fig. S3). The effect of these minerals became negligible at 350 °C.

Regarding phosphate reduction to phosphite, the type of reducing agents (Fe^{2+}, and H_2) as well as temperature exerted strong controls. Under N_2 flow-through conditions, where Fe^{2+} was the reducing agent, phosphite was not detected at 80–200 °C, but it became detectable at 350 °C (yield 0.075%). When H_2 was added, phosphite was detectable at 200 °C, particularly in the presence of other minerals, reflecting the ability of H_2 to act as an additional reducing agent (Fig. 3D, Supplementary Fig. S4). On the other hand, a direct comparison between 200 and 300 °C N_2 flow, between 200 °C and 350 °C static H_2, and between 600 and 700 °C H_2-flow experiments shows a phosphite yield increase of 75, 15, and 100 times, respectively, revealing enhanced reduction at elevated temperature in each pair (Fig. 3D–F). We stress that the 600 and 700 °C experiments were conducted in a different setup and were therefore not directly comparable to those at ≤350 °C, but the temperature dependence was confirmed.

The Fe-/Ni-/Cr-bearing minerals also impacted the phosphite yield, and the effect of these minerals is dependent on temperature. At 200 °C, the highest phosphite yield of 0.004% was obtained in the presence of chromite (Fig. 3D). Lower yields of 0.002% were obtained in the presence of Ni and Ni_3S_2. Phosphite was not detected in experiments without these minerals and when magnetite or pyrite were used (Fig. 3D). At 350 °C, the maximum yield of 0.058% was obtained when Ni and Ni+Fe were used as catalyst (Fig. 3E). Ni_3S_2- and chromite-bearing samples showed moderate yields of 0.015% and 0.008%, respectively, while magnetite had no effect (Fig. 3E).

For the thermodynamic modeling, we note that specific thermodynamic data for Fe-P phases (polyphosphates and reduced P compounds) are unavailable, and thus the modeling is constructed for the simpler H-P-O system (Fig. 4). Therefore, the graphs are illustrative but not exactly reflective of the experiments. For example, the calculations suggest the

Table 2 | Summary of the experimental results

T [°C]	Exp. No.	Mineralogy (XRD)	Aqueous P % (NMR, IC, IC-ICPMS)						
				Pi	P(III)	PPi	PPPi	PPPPi+	PPPc/ PPPPc
Evaporation stage									
85	E1	Rokuenite ($FeCl_2.2H_2O$), Halite (NaCl), Amorphous $Fe_3(PO_4)_2.xH_2O$		97.225	BDL	**2.775**	BDL	BDL	BDL
60	E2	Rokuenite, Halite, Amorphous $Fe_3(PO_4)_2.xH_2O$		87.094	BDL	**1.710**	BDL	BDL	BDL
Static atmosphere heating:									
200	S1 A S1 B	Rokuenite, Halite, Amorphous $Fe_3(PO_4)_2.xH_2O$	A B	100 84.769	BDL BDL	BDL **15.105**	BDL **0.125**	BDL BDL	BDL BDL
200	S2 A S2 B	A - Rokuenite, Halite, Amorphous $Fe_3(PO_4)_2.xH_2O$ B - Rokuenite (minor), Halite, Amorphous $Fe_3(PO_4)_2.xH_2O$	A B	100 67.496	BDL NA	NA **32.504**	NA NA	NA NA	NA NA
200	S3 A-G	A - G: Rokuenite, Halite, Amorphous $Fe_3(PO_4)_2.xH_2O$, respective catalysts as provided	A	97.393	BDL	**2.603**	**0.003**	BDL	BDL
			B B$	99.091 97.295	BDL BDL	**0.908** **2.705**	**0.002** BDL	BDL BDL	BDL BDL
			C$	35.116	BDL	**53.717**	**9.290**	**1.877**	BDL
			D	82.548	**0.002**	**17.275**	**0.175**	BDL	BDL
			E E$	80.823 45.911	**0.002** BDL	**18.828** **44.081**	**0.347** **8.650**	BDL **1.358**	BDL BDL
			F	68.986	**0.003**	**30.025**	**0.986**	BDL	BDL
			G	88.361	**0.004**	**11.635**	BDL	BDL	BDL
350	S4	$FeCl_2$, rokuenite, Fe-hydroxide ($Fe(OH)_2$), $FeO(PO_4)$ (?), $NaFePO_4$ (?), halite, other unidentified phases		100	NA	BDL	BDL	BDL	BDL
350	S5 A-E	A - E: $FeCl_2$, rokuenite, Fe-hydroxide ($Fe(OH)_2$), $FeO(PO_4)$ (?), $NaFePO_4$ (?), halite, other unidentified phases A, C-E: respective catalysts as provided; B: Ni	A	100	BDL	BDL	BDL	BDL	BDL
			B	99.985	**0.015**	BDL	BDL	BDL	BDL
			C	99.942	**0.058**	BDL	BDL	BDL	BDL
			D	99.992	**0.008**	BDL	BDL	BDL	BDL
			E	99.969	**0.031**	BDL	BDL	BDL	BDL
Flow-through heating:									
170	F1	Halite, Amorphous $FePO_4.xH_2O$, other unidentified amorphous condensed phosphate phase(s) of Fe		30.128 30.630	BDL BDL	**19.181** **60.636**	**24.359** **4.952**	**26.332** BDL	BDL **3.780/0.299***
200	F2 A F2 B	Halite, Amorphous $FePO_4.xH_2O$, other amorphous condensed phosphate phase(s) of Fe, olivine (only B)	A	56.259	BDL	**38.446**	**4.611**	**1.140**	BDL
			B	44.868	BDL	**48.037**	**5.788**	**1.961**	BDL
350	F3	$FeCl_2$, rokuenite, Fe-hydroxide ($Fe(OH)_2$), $FeO(PO_4)$ (?), $NaFePO_4$ (?), halite, other unidentified phases		99.735	**0.075**	**0.19**	BDL	BDL	BDL
600	F4	Fe, NaCl, NaFePO4 (?), $Fe(PO_4)O_3$ (?)		99.991	**0.009**	BDL	BDL	BDL	BDL
700	F5	Fe, $Fe_3(PO_4)_2$		99.899	**0.101**	BDL	BDL	BDL	BDL

Pi: phosphate, P(III): phosphite, PPi: pyrophosphate, PPPi: triphosphate, PPPPi + : tetra- and other higher order phosphates, PPPc: trimetaphosphate, PPPPc: tetrametaphosphate; *Measured after 50 days; NA: Not analyzed; BDL: below detection limit 0.001% for P(III) and 0.05% for polyphosphates; Phases with marked with "?"only tentatively identified.

stability of PPi up to 700 °C in the H-P-O system, which is not the case in the experiments (Figs. 2, 4A). However, the thermodynamic model predicts that polymerization occurs best at low water activity and reduction is best facilitated by high H_2, consistent with the experiments (Fig. 4A). The modeling also suggests that formation of cyclophosphates may be feasible at lower temperatures if the water activity is low (Fig. 4B).

Discussion

New constraints on phosphate reduction and polymerization

Our results provide several new insights into the formation of reactive P species that may have fueled prebiotic chemistry on the early Earth:

(1) Polymerization of phosphate in P-rich ferruginous conditions maximises at moderate temperature and becomes limited at lower and high temperatures. Our results disprove the hypothesis of increasing polymerization yield with increasing temperatures (above 200 °C)[11] and suggest that moderate temperatures (80–200 °C) are optimal for polymerization in the Fe-PO_4 system. The reason for the temperature dependence is likely linked to Fe-mineralogy. Previous studies noted that polyphosphates tend to crystallize as amorphous phases[36,43], but we noted the formation of crystalline phosphates at temperatures ≥350 °C (Fig. 1), which may explain lower polymerization yields. Also, the Fe-phosphate precursor likely has an impact. A previous study found that vivianite loses water sequentially at 100–500 °C but does not form any polymers[44]. Likewise, polymerization was not observed when we conducted experiments with vivianite at 200 °C (not shown). Instead, a meta-stable amorphous Fe-phosphate phase ($Fe_3(PO_4)_2.xH_2O$), as generated during evaporation in our experiments, may be a prerequisite for polymerization.

(2) Polymerization yields increase in the presence of Fe-/Ni-/Cr-bearing minerals except for magnetite, which decreases polymerization. It has been previously shown that silica stabilize phosphate on its surface, thereby facilitating polymerization upon subsequent heating[40,41]. Most likely, amorphous Fe-phosphate precipitated on the surface of these minerals (except for magnetite), which brought the phosphate molecules closer together, enhancing Pi-Pi interaction and polymerization. In the case of magnetite, which contains Fe^{3+} and is known to strongly absorb phosphate[45], the interaction between the surface and Pi might have overpowered the Pi-Pi interaction, thereby reducing the Pi-Pi interaction and the polymerization yield. Alternatively, magnetite might have enhanced the

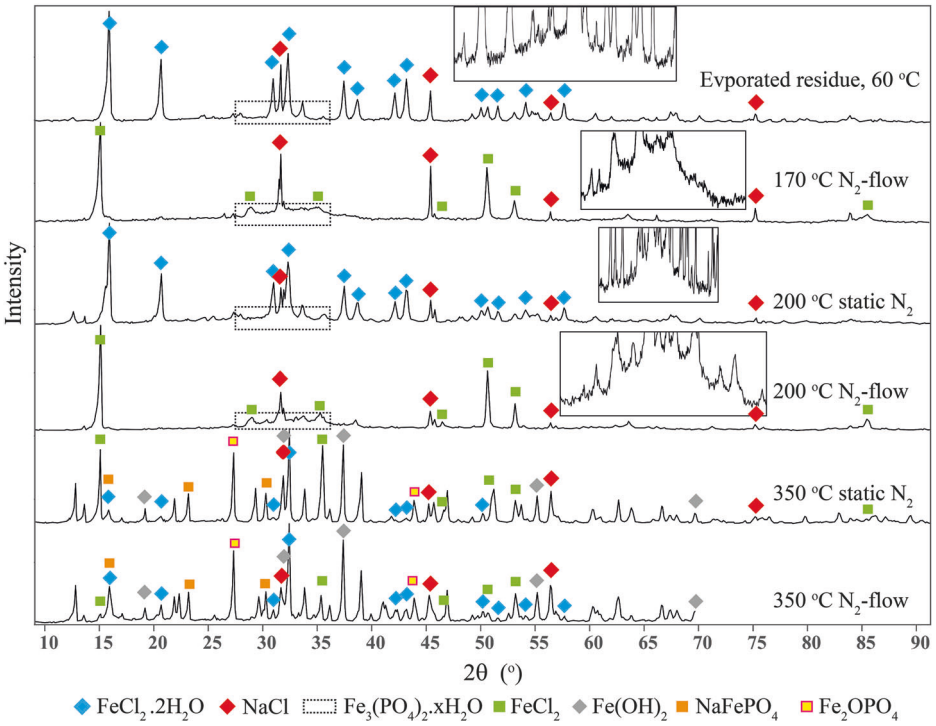

Fig. 1 | XRD data of selected experimental products. The broad peak from 27 to 35 ° (2θ) is shown in the dotted boxes and some representative broad peaks are enlarged in the inset graphs, which represent amorphous $Fe_3(PO_4)_2{\cdot}xH_2O$ (and possibly other amorphous polyphosphate phases for the 170 °C and 200 °C N_2 flow-through experiments). At 350 °C, all phases are crystalline; and amorphous $Fe_3(PO_4)_2{\cdot}xH_2O$ appears to be unstable at this temperature. Some phases in the 200 and 350 °C residues could not be unambiguously identified (e.g., the presence of $NaFePO_4$ and Fe_2OPO_4 is speculative).

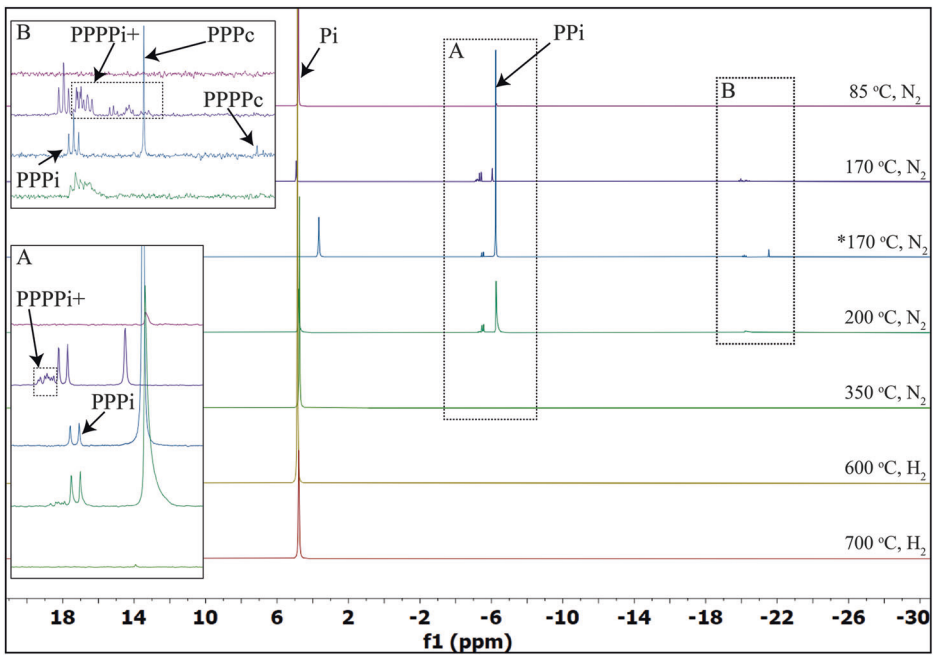

Fig. 2 | Proton decoupled ^{31}P NMR data of EDTA-NaOH extracts. Box A and B are enlarged in inset graphs. Chemical shifts are presented relative to an 85% H_3PO_4 standard having a chemical shift of 0 ppm. Pi and PPi have chemical shifts of 5 and −6.2, respectively. PPPi appears as doublet in between −5.3 and −5.4 ppm and as a triplet in between −19.7 and −20.0 ppm. PPPPi+ has multiple peaks in between −5.1 to −5.3 ppm and between −20.1 and −21.2 ppm. PPPc and PPPPc have single peaks at −21.5 ppm and −23.7 ppm, respectively. Slight variation in the chemical shift is due to the pH of the solution (we noticed that the dependency of Pi on pH is more intense compared to other condensed P species). All analyses were performed within 1–2 days after the experiments, except for the sample marked with an asterisk, which was stored at room temperature for 50 days before analysis.

hydrolysis of polyphosphates in the EDTA-NaOH solution, as has been described for other Fe-oxides[46], lowering polymerization yields.

(3) Our data provide the first evidence that cyclophosphates and long-chain polyphosphates (up to pentaphosphate) can form in naturally relevant ferruginous conditions. The long-chain phosphates converted into cyclophosphates (PPPc and PPPPc) at room temperature in contrast to previous reports of the same happening at 100 °C in a P_4O_{10}-rich solution[38]. Higher thermodynamic stability of cyclophosphates compared to linear phosphates suggests that cyclization can occur spontaneously (Fig. 4B). Our PPPc yield is similar to that reported in high-temperature volcanic environments[38], in phosphide oxidation reactions[39], or in the ammonium phosphate ± urea system[37], suggesting an additional and perhaps more naturally widespread route for PPPc formation on the early Earth. PPPPc minerals have been hypothesized to be the product of pyrolytic oxidation of metallic phosphides at >300–400 °C, and the mechanism might have formed cyclophosphates on the early Earth[47]. Our data reveal an additional route at lower temperatures that does not require precursor phosphide minerals.

(4) Iron(II)-induced phosphate reduction to phosphite is more difficult than previously reported[11], but on the other hand, some degree of Fe(II)- and

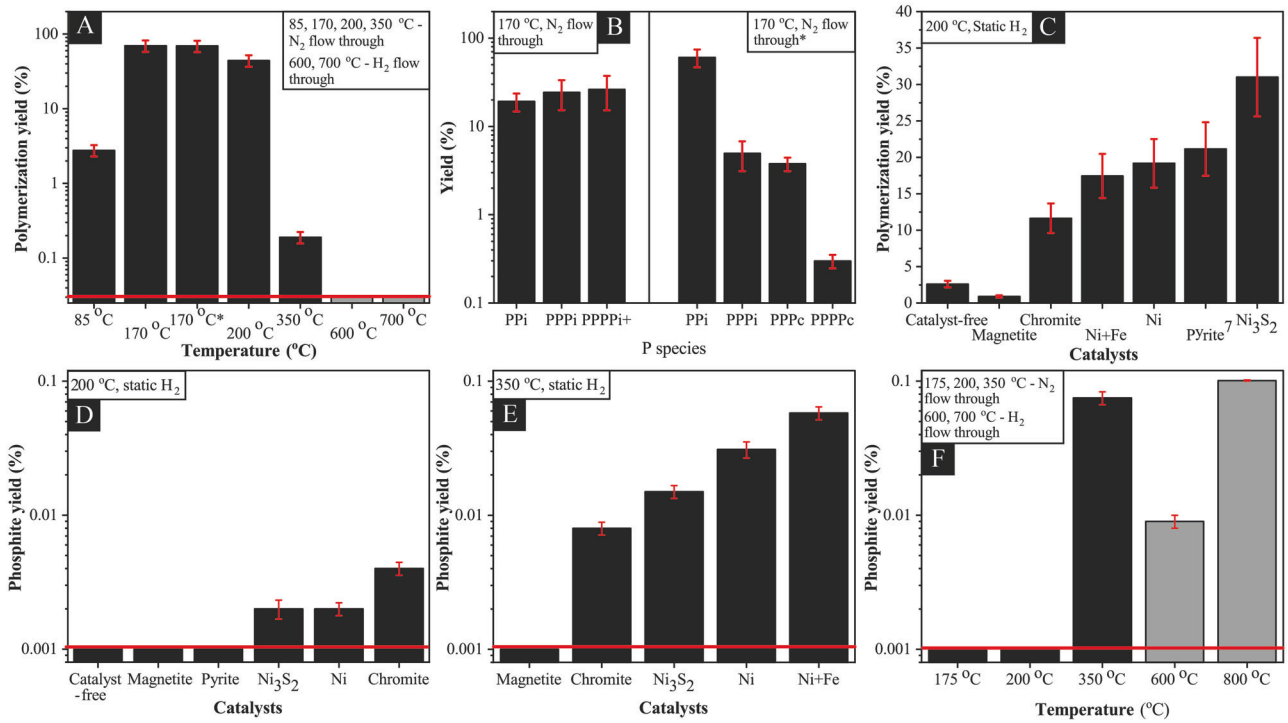

Fig. 3 | Experimental polymerization and reduction yields relative to the initial phosphate input. Red horizontal line = detection limit of the IC-ICPMS method. Typical error of repeat experiments or in measurements is given where P species are detected. 600 and 700 °C experiments were conducted in a tube furnace unlike other experiments conducted in hydrothermal reactors and marked with gray column. **A** Polymerization yield as a function of temperature under gas flow-through conditions. **B** Change in the proportions of differing condensed species formed at 170 °C after 50 days of storage at room temperature (labeled 170 °C*). Proportions of PPi, PPPc, and PPPPc have increased in concomitant reduction of PPPi and PPPPi+. **C** Polymerization yield as a function of catalysts (200 °C, H_2-static experiments). **D** Reduction yield in 200 °C H_2-static experiments. **E** Reduction yield in 300 °C H_2-static experiments. **F** Phosphite yields as a function of temperature in the absence of catalysts with N_2 flow (175–350 °C) and H_2 flow (600–700 °C).

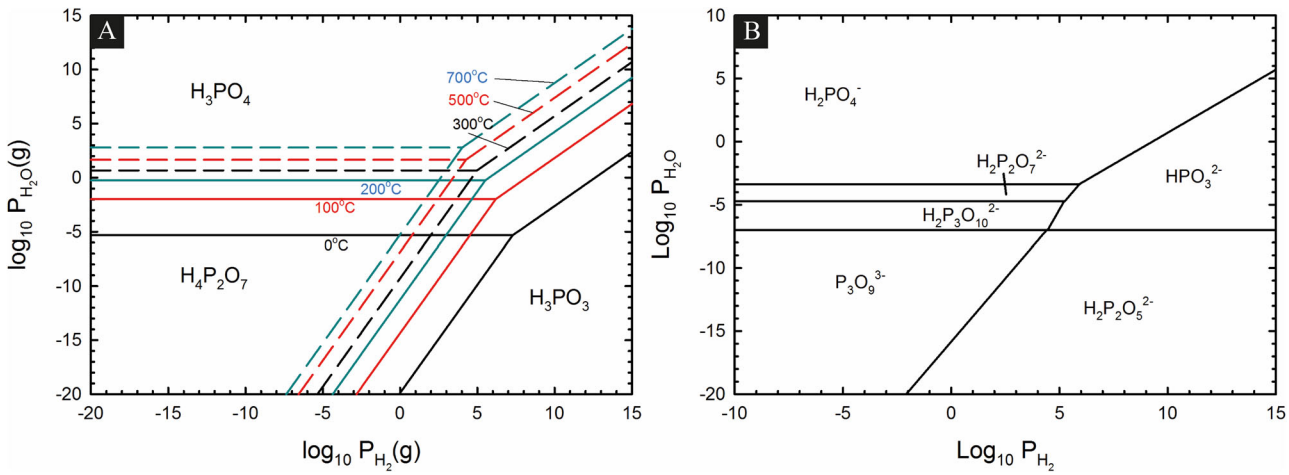

Fig. 4 | Equilibrium calculations for phosphate polymerization and reduction. Pressures are in atm. The calculations are based on the data from Pasek[69] at 25 °C and from 0 to 700 °C using data from HSC Chemistry[70]. In all calculations, the activity of the P species on a given line was assumed to be equal. **A** Using HSC Chemistry, the predicted domains where phosphate (as H_3PO_4) polymerizes into pyrophosphate ($H_4P_2O_7$) and phosphite (as H_3PO_3) is a function of H_2O and H_2 activity. It is also changed by the temperature of the system, which in this graph changes from 0 to 700°C. These species were all considered as acids, to avoid pH effects. **B** Using data from Pasek[69] on prebiotic phosphorylating agents, the regions where various polyphosphates, phosphite, and pyrophosphate would be expected to dominate at pH 7 is likewise a function of H_2O and H_2 activity. Notably, when linear polyphosphates become larger than 3–4 phosphate units, cyclization is spontaneous.

H_2-induced reduction can occur over a wider temperature range (200–700 °C) than previously explored. Herschy et al.[11] obtained a Fe(II)-induced reduction yield of 4% at 180 °C while we did not see any detectable phosphite at 170–200 °C although experimental setups were broadly similar. Our maximum yield was 0.1% at 700 °C, which probably is a combined effect of Fe(II)- and H_2-induced reduction. Herschy et al.'s (2018)[11] thermodynamic calculations predicted that phosphite yields increase with temperature and Fe^{2+} is a more effective reductant than H_2 at

100–500 °C[11]. Our data support the former conclusion and show that the latter occurs at temperatures around 350 °C. However, at 200 °C, H_2 appeared to be a better reducing agent compared to Fe^{2+}, particularly if Ni, Ni-sulfide, and chromite are present. These minerals are known to catalyze the reduction of carbon and nitrogen[48] and may have a similar catalytic effect on phosphate reduction. If so, it would indicate kinetic inhibition of phosphate reduction in the absence of these catalysts. Such a kinetic effect may also explain why elevated temperatures results in higher reduction yields, as this may help overcome the kinetic barrier. One possible reason for absence of a catalytic effect in magnetite may be the presence of Fe^{3+}, which perhaps changes the redox state of the Fe-P system in favor of phosphate[11].

(5) Lastly, the formation of phosphite is not precluded by hydrous mineral phases. Phosphite is thermodynamically stable under highly reducing conditions below the stability field of water, that favor H_2 over H_2O[10]. This likely explains the temperature-dependence of phosphite formation, as H_2O is lost with increasing temperature. However, some $Fe(OH)_2$ and $FeCl_2{\cdot}2H_2O$ were still present in experiments where phosphite formed, indicating that phosphite can form as long as residual water is locked into minerals.

Implications for early Earth

The conditions we explored here are relevant to a range of settings on the early Earth and can therefore help to constrain the availability of reactive P species for the origin and early evolution of life. The formation of phosphite induced by concomitant Fe(II) oxidation can take place during burial or contact metamorphism at 350 °C or higher in P-bearing ferruginous sediments, which would have been widespread in the Archean, when the ocean was ferruginous with possibly millimolar concentrations of Fe^{2+} [49,50]. Herschy et al.[11] reported phosphite from Archean Isua and Akilia rocks in Greenland (3.7-3.8Ga) and provided several possibilities for its origin, including diagenesis and metamorphism. As we see a strong correlation between the phosphite yield and temperature in our experiments, and as the Isua and Akilia rocks went through amphibolite and granulite facies metamorphism, respectively, we suggest that a significant part of the phosphite might have been produced during metamorphism, i.e., at higher temperatures than that explored experimentally by Herschy et al.[11]. Importantly, the phosphite/phosphate ratio is higher in granulite facies Akilia rocks (3.24) compared to amphibolite facies Isua rocks (0.31–0.84), which further supports the temperature dependence of phosphite formation. In these localities, phosphate may have co-precipitated with iron[3] and formed Fe-phosphate phase during diagenesis[50–52]. Subsequently, Fe(II)-induced reduction of phosphate may have happened during metamorphic heating. We note that our and the previously reported experimental phosphite yield are significantly lower than that in natural rocks, which further attests to the kinetic barrier of the reduction reaction. This barrier is likely overcome with time. While our experiments were very P-rich, high P concentrations are probably not required to drive phosphate reduction, as long as conditions are sufficiently hot and anhydrous and reductants such as Fe(II) or H_2 are present. In fact, the formation of amorphous Fe-phosphate, most likely the type that formed in these experiments, is preferred during diagenesis in ferruginous conditions with low P concentrations[52]. Hence this reaction could have occurred in sediments deposited in marine environments, which were perhaps P-depleted[53], but Fe^{2+}-enriched[49] on the early Earth.

Our results provide an explanation for the detection of phosphite in serpentinite[35] and suggest that it may be a common occurrence. Serpentinizing environments are highly reducing environments that produce a significant amount of H_2 as well as metallic nickel and iron as awaruite along with nickel sulfide and magnetite[54,55]. Our results provide experimental evidence that in the presence of Ni, Fe, nickel sulfide, and chromite (usually present as a primary phase in ultramafic rocks), H_2 may act as the main reducing agent for phosphate during serpentinization, particularly at temperatures below 350 °C in which H_2 is a better reducing agent compared to Fe^{2+}. H_2 production during serpentinization can be variable but it has been shown to reduce C into CH_4 via Fisher-Tropsch-Type reaction during serpentinization[56], and may thus be sufficient for phosphate reduction as well. Dry conditions are required for phosphate reduction, consistent with serpentinization settings where H_2O is removed during conversion of olivine into serpentine minerals[55,57]. We speculate that such dry conditions can be achieved in deeper part of the crust where the serpentinization may happen at high temperatures at very low water:rock ratios, particularly at micron scale. At comparatively lower depths, where the water:rock ratio may be higher, the reduction of phosphate into phosphite is perhaps suppressed. We further note that magnetite may interrupt the formation of phosphite while chromite, metallic Ni, and Ni-sulfide may accelerate it, which may suggest that H_2-induced reduction during serpentinization can be heterogeneous. The presence of water (i.e., high water:solid ratio) or magnetite may explain the absence of phosphite in certain serpentinite muds reported in Pasek et al.[35].

Regarding phosphate polymerization on the prebiotic Earth, relatively high initial phosphate concentrations are probably required. Dissolved phosphate concentrations in the Archean ocean are debated with estimates varying from sub-micromolar levels[3] to up to 1 mM, i.e. 1000 times higher than today[9]. If seawater phosphate levels were low, then volcanic lakes and hot-spring pools may have offered an alternative setting with high dissolved phosphate levels, like their modern analogs such as Lake Magadi in Africa and thermal springs on the Kamchatka Peninsula[7,58]. Here, volcanically-heated subaerial hot-spring environments with lakes and hydrothermal pools[59,60] may have offered ideal conditions for phosphate polymerization as identified in our experiments (Fig. 5). As noted earlier, the solubility of bioessential micronutrients such as Cu and Zn may be low in high-pH lakes, but once polyphosphates are formed, they may be exported to other environments with a higher overall metal inventory. The abundance and extent of these subaerial hot-spring environments on the early Earth are unknown; however, their occurrence is recorded in 3.5 Ga rocks on the Pilbara Craton[59], indicating the natural relevance of this type of environment. The concentration of dissolved phosphate in such settings is dependent on physicochemical conditions, particularly pH, bivalent cations and carbonate concentrations, with alkaline conditions favouring phosphate enrichment[7]. However, acidic hot spring pools, such as those on the modern Kamchatka Peninsula, also show high phosphate levels reaching up to 1 mM along with high concentration of Fe (reaching an Fe:P ratio up to 8)[58], a condition that mimics our experiment. Modern-day volcanic lakes and hydrothermal pools experience wetting-drying cycles and variability in temperature and pH[61], which would likely also have happened on the early Earth. Evaporation enriches dissolved phosphate[7,9,58] and potentially precipitates Fe-phosphate[50,52], similar to what we observed in the evaporation stage (Fig. 5B). These lakes or pools likely contained other bivalent metals such as Ca, Mg, and other anions such as carbonate and silica, which might have impacted the mineralogy of the evaporated residue. Although exploring these parameters was beyond the scope of the study, formation of Fe-PO_4 phases is likely, particularly because volcanic environments are typically Fe-enriched and formation of amorphous Fe-PO_4 may take place in low-P ferruginous conditions conducive to greenalite formation[50,52]. Moreover, the formation of Fe-phosphate may happen after deposition and during diagenesis as observed in ferruginous rocks[51,52]. Subsequently, magmatic intrusions or lava flows could have triggered thermal metamorphism of these sediments and evaporites[29], producing the wealth of polyphosphate species that we observed in the experiments. Mineral catalysts including magnetite, chromite, pyrite, Ni, Fe, and Ni-sulfide derived from the (un-)altered bedrocks could have accumulated in these lakes or pools[62], which likely enhanced the polymerization process during the thermal heating stage. Importantly, phosphite formation may also occur in the same environment along with polyphosphates if temperatures reached above 200 °C and would have enhanced if H_2 produced by hydrothermal alteration of (ultra-)mafic rocks[55] was available. Furthermore, in saline lake environments, solar heating alone may achieve temperatures as high as 95 °C[63]. In such cases, evaporation of phosphate-rich solution may lead to some degree of polymerization, enhanced by the catalyst minerals that we used in our experiments. In summary, temperature gradients, reducing

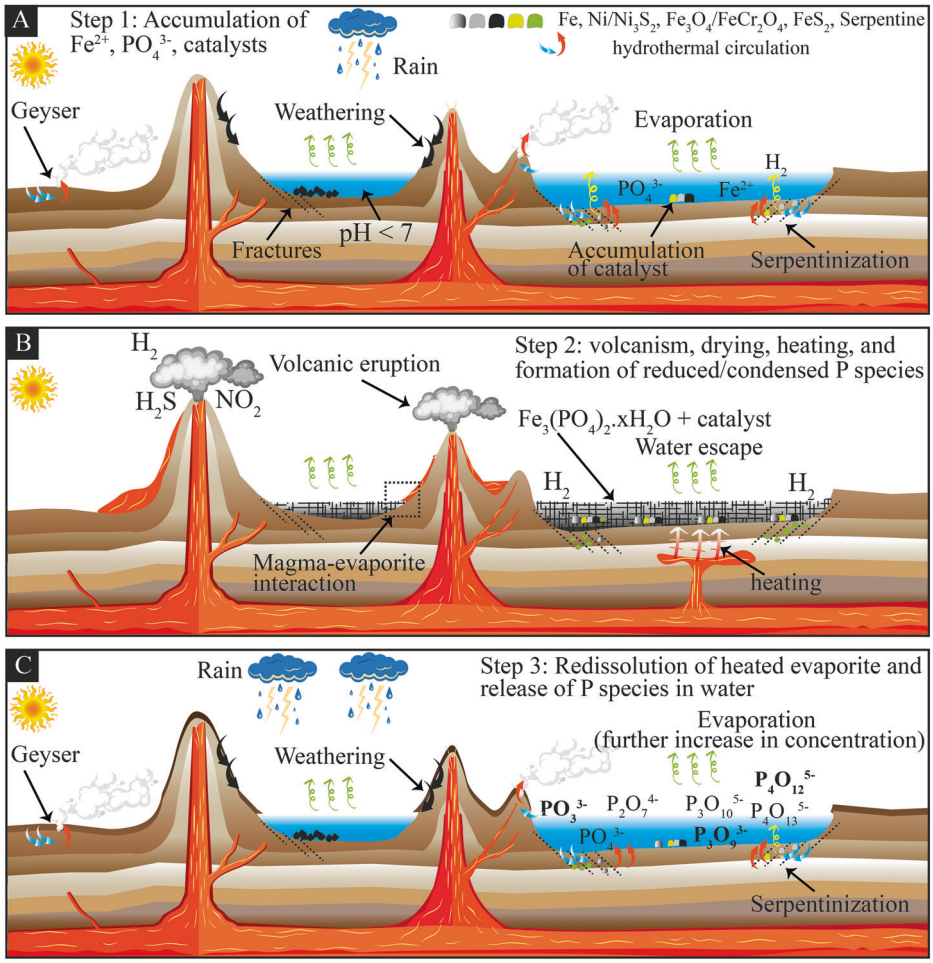

Fig. 5 | Schematic of the proposed mechanism of phosphate reduction and polymerization on early Earth. A Possible routes of phosphate, Fe^{2+}, and catalyst mineral accumulation in wet-dry pools by hydrothermal circulation and rock weathering[29,32,58,59,62]. **B** Formation of evaporites or sediments containing $Fe_3(PO_4)_2.xH_2O$ in these pools. Thermal metamorphism may ensue as a consequence of magmatic heating, driving phosphate polymerization and/or reduction, depending on temperature, reductants, and catalyst availability. **C** Subsequent re-dissolution of the products and release of polymerized and reduced P species back into the environment[11,43].

agents (Fe(II) and possibly H_2), and potential catalysts make hot-spring settings and saline lakes attractive for phosphate reduction and polymerization on the early Earth.

Liberation of reduced and polymerized P species into water is the next important step for phosphorylation reactions for the origin of life. Phosphite is ca. 1000 times more soluble than phosphate[11], and hence hydrothermal rehydration of metamorphosed ferruginous sediments that have undergone phosphate reduction would have created a plausible pathway for dissolved phosphite back into the environment (Fig. 5C). Similarly, phosphite produced during serpentinization may be released into water as evident by the lower P content in altered ultramafic rocks compared to its unaltered precursor[35]. On the other hand, the solubility of the various polyphosphate species in natural fluids is not well known, especially under ferruginous conditions. However, the presence of dissolved H_2S, which may be abundant in volcanic settings, can enhance polyphosphate solubility by scavenging Fe^{2+} as iron sulfides[43]. Additionally, Fe-chelating organics, such as citrate, which were possibly present on the prebiotic Earth[64], could have enhanced the release of polyphosphates from meta-sediments or meta-evaporites (Fig. 5C). Upon re-dissolution, straight-chain polyphosphates undergo hydrolysis and transform into shorter chain (poly)phosphates and cyclophosphates, which subsequently hydrolyze into phosphate[36,43,65,66]. Previous studies suggest that the half-life of these poly- and cyclophosphates in water may vary from days to thousands of years, depending on pH, temperature, and the presence of bivalent cations[36,65,66]; and this time may be sufficient for some phosphorylation reactions[5,6,23]. If a sufficient amount of the straight-chain polyphosphates and cyclophosphates accumulated in a pool or lake that contained organic compounds including urea and/or fomamide, subsequent wet-dry cycles may produce a wealth of phosphorylated compounds via different reaction routes. For example, if borate were also present along with ribose in these settings, then nucleotide formation via reactions between ribose-phosphate and nucleobase is likely[20,21]. In the absence of borate, nucleotide formation via reactions between nucleosides and reactive P-species, including PP, PPP, PPPc, PPPPc, and phosphite, could have occurred[6,16–19]. Furthermore, PPPc may transform into amidotriphosphate or monoamidophosphate upon reaction with dissolved ammonium, which may subsequently facilitate nucleoside phosphorylation[25,27,28]. To summarize, the alternative P species that were formed in our experiments can be useful for the prebiotic phosphorylation of organic molecules, which is key step for the origin of life.

In conclusion, we find that thermal metamorphic processes on ferruginous sediments and evaporites precipitated in phosphate-rich volcanic environments on the early Earth and possibly on Mars could have created an important route for the formation of reactive P species, including polyphosphates and phosphite. Our findings include a naturally relevant pathway for the formation of cyclophosphates, which may have been particularly reactive towards organic matter in prebiotic reactions[23]. Phosphite formation may have occurred also in other P-depleted metamorphic settings and during serpentinization, and it may have been accelerated in the presence of catalytic minerals. Our identified polymerization pathways may have been more common than previously proposed alternatives and may therefore represent a new environmental solution to the P-problem in the origin of life.

Materials and methods

Experiments

Acid-washed and baked (500 °C) glass containers were used in all the stages of the experiments and subsequent sampling. $FeCl_2.4H_2O$, NaH_2PO_4, and catalysts (Ni, Fe, Ni_3S_2, Ni+Fe (3:1), FeS_2, Fe_3O_4, $FeCr_2O_4$) were added in a

molar ratio of 3:1:0.5 (or 1) in deoxygenated, deionized water with a pH of 4 to produce weakly acidic solution representative of hydrothermal pools (this design was initially adopted from Herschy et al.[11]). Control experiments without catalysts were also performed. Among these chemicals, $FeCl_2.4H_2O$, NaH_2PO_4, Ni, Fe, Ni_3S_2, and Fe_3O_4 were synthetic and bought from Fisher Scientific while FeS_2 and $FeCr_2O_4$ are natural samples. All the catalysts were used in powdered form and analyzed using XRD before experiments. We did not see any impurity in them except for chromite, which contains minor olivine. More importantly, we did not see any detectable amount of phosphite or polyphosphate in any of the starting materials including the catalysts. In a typical experiment, we took 400 ml of water and added 1 M HCl dropwise to make a pH of 4. The pH was measured using the Thermo Scientific pH paper strips. Then, we added 2.3857 g $FeCl_2.4H_2O$, 0.47992 gm, NaH_2PO_4 and the known amount of catalyst (weight equivalent of 5 or 10 mM) to make a solution containing 30 mM Fe(II) and 10 mM phosphate. In a few experiment, we took 300 mM Fe(II) and 100 mM phosphate at this stage; however, we did not see any difference in the products (tested in XRD) data after evaporation. The solution was stirred for 40 minutes in anoxic conditions (purged with N_2 gas) that led to the dissolution of $FeCl_2$ and phosphate salts. The Fe-/Ni-/Cr-bearing minerals remained the same before and after the evaporation stage as evident from XRD data. We cannot completely rule out the possibility that there could be minor dissolution of these catalysts, but the bulk of the mass remained in a solid state based on visual inspection. In one experiment (700 °C, described below), we used $NH_4H_2PO_4$ (Fisher Scientific) instead of NaH_2PO_4 as the phosphate source.

The solution was then loaded into a Berghof reactor equipped with a heating mantle, a K-type thermocouple for temperature monitoring, gas lines (H_2 and N_2), and a vacuum pump (Supplementary Fig. S1A). After loading the solution, an anoxic environment was created inside the reactor using the vacuum pump and by flushing the system with N_2 followed by evacuation (5 cycles of N_2 flushing and evacuation). The heat source was turned on and the solution was evaporated at 60–65 °C either under vacuum or constant N_2-flow to maintain anoxic conditions to replicate the evaporation of those hydrothermal pools under an anoxic Archean atmosphere. The evaporated residue was then cooled down to room temperature and then quickly crushed in an agate mortar and pestle (see Herschy et al.[11]) and reloaded into the reactor (Berghof or Parr) to be dry-heated for up to 7 days at temperatures of 170, 200, and 350 °C, either in static or flow-through N_2/H_2 environments (see Table 1 for the initial conditions of the experiments). In two gas-locked experiments, the gas was briefly vented from the reactor after 3 h or 24 h, respectively. This step was performed to get rid of water that would have built up within the headspace of the reactor within those first few hours. This experiment was done to further explore the effect of water on phosphate reduction and polymerization[11,43].

Two high temperature (600 and 700 °C), H_2-flow (5% H_2 + 95% N_2; flow rate of 20 ml/min) experiments were performed in a tube furnace where the evaporated residue was loaded into an alumina boat, a K-type thermocouple was used to control temperature, and a ramp of 5 °C/min was used to reach the desired temperature, which was maintained for either 1 hour (700 °C) or 2 h (600 °C), followed at 5 °C/min (Supplementary Fig. S1B). Heated residues were cooled down and stored in N_2-environments to avoid oxidation before subsequent analysis.

Solid characterization using powder X-ray diffraction (PXRD)

The evaporated and heated solids were powdered with pestle & mortar and part of them was loaded into 0.5 mm capillary tubes for XRD analysis. The PXRD patterns were recorded on a STOE STADIP diffractometer using Mo Kα1 radiation at room temperature from 2.5° to 35° (2θ) with a scan rate of 2.5–3.5° (2θ)/step in capillary Debye-Scherrer mode. The PXRD data were compared to solids in the Inorganic Crystal Structure Database (ICSD) for phase identification using the Crystal Diffract software (version 6.9.3).

Quantification of P species in the solution

Part of the solid was treated with Ethylenediaminetetraacetic acid-sodium hydroxide (0.05 M EDTA and 0.25 M NaOH solutions were prepared separately and mixed in 1:4 ratio) solution[35] maintaining a solid:solution ratio of 1:200 or 1:50 for 3–15 h. Higher solution volume was used for experiments where Ni-/Fe-/Cr-bearing minerals were not used to make sure to extract maximum amount of P and get rid of all the dissolved Fe^{2+}. After this treatment, an additional 0 to 30% EDTA-NAOH solution with respect to the initial volume was added to the solutions to precipitate all the remaining Fe^{2+}. This step is essential because iron may precipitate as oxides in the separation column of the ion chromatograph (IC) and bind phosphate by adsorption, thereby impacting analytical quality. It also hampers the magnetic resonance spectrum in nuclear magnetic resonance (NMR). The solution was centrifuged several times to obtain a clear solution where all iron had precipitated to the bottom of the centrifuge tube.

For the phosphite measurements, we used the IC-ICPMS set-up of Baidya and Stüeken[67] modified from Ivey et al.[68]. A Thermo Scientific Dionex ICS-6000 ion chromatograph equipped with a Dionex AS-AP autosampler, a 25 mm Dionex IonPac AS17-C separation column (2 mm bore), a 25 mm Dionex IonPac AG17-G guard column (2 mm bore), and a Dionex ADRS 600 2 mm Suppressor Module was used to separate the phosphite fraction from phosphate and other P species in the solution. The flow rate was held constant at 0.5 ml/min while the concentration of the KOH eluent solution was ramped up from 1 mM to 40 mM over 20 min and then this maximum KOH concentration was held constant for another 20 min. This IC configuration was capable of separating phosphite from phosphate and pyrophosphate. Suppressor outlet of the IC was physically connected to 1 ml/min nebulizer attached to the spray chamber (Scott model; quartz glass) of a Thermo Scientific Element2 ICP-MS operated in medium resolution mode to separate ^{31}P from HNO interferences with the same mass. Data were collected in the ICP-MS for 3 minutes with a chromatographic method centered on the m/z of ^{31}P (one minute for monitoring the pre-phosphite background, one minute for the phosphite peak, and one minute for monitoring post-phosphite background). The chromatographic data from the ICP-MS were smoothened with the Origin Lab software, using the fast furrier transform filter with a points-of-window value of 5–6, and the peak area under the curve was used for quantification of phosphorus. A calibration curve was generated using phosphite standards ($Na_2HPO_3.5H_2O$; Fisher Scientific®) ranging from 0.1 ppb to 50 ppb P and used to calculate phosphite concentration in the experimental samples. The detection limit of the IC-ICPMS was <0.1 ppb. This corresponds to ca. 0.001% of the total phosphorus present in the experiment.

Other polyphosphate species including pyrophosphate (PPi), triphosphate (PPPi), trimetaphosphate (PPPc)[38], tetrametaphosphate (PPPPc)[38], tetra- and other higher order polyphosphates (PPPPi+) were measured on a Bruker AVIII 500 MHz nuclear magnetic resonance (NMR) instrument equipped with a nitrogen-cooled broadband cryoprobe. Sample solutions and standards were added with 10-20% D_2O to make a total volume of 0.6 ml and analyzed in proton-decoupled mode with 3000-7000 scans. The ^{31}P chemical shifts are referenced to phosphoric acid having a chemical shift of 0δ. Standards of known concentrations (0.1 ppm to 800 ppm phosphorus, generated from; $K_4P_2O_7$, $Na_5P_3O_{10}$, and $Na_5P_3O_9$; Fisher Scientific) were analysed to determine the detection limit and build calibration curves for each P species. We were not able to create calibration curves for PPPPc and PPPPi+ because relevant standards could not be purchased. Instead, we tentatively used the calibration curve of PPPi. The detection limits of the various polyphosphate species was 0.05% relative to the total phosphorus present in the experiment.

Thermodynamic modeling

Thermodynamic relationships between various species of H-P-O compounds were determined using data from Pasek [69] and from data in the HSC Chemistry program[70]. For the latter, the balanced reactions involving H_3PO_4(aq), $H_4P_2O_7$(aq), and H_3PO_3(aq) were constructed. From these, the

partial pressures of $H_2O(g)$ and $H_2(g)$ were determined for the line of equivalence of each as a function of temperature (e.g., where $[H_3PO_4] = [H_4P_2O_7]$), from 0 to 700 °C. All species were considered to be aqueous solvated acids even at high temperature, despite the fact that the system was investigated under dry conditions, mainly because the data was most available for these species. Because all three species were solvated, error introduced by operating outside the range of temperature of liquid water stability should be smaller than if a species were present as a anhydrous acid (e.g., H_3PO_4).

Using the shape of this diagram, data from Pasek [69], which also includes triphosphate, cyclic triphosphate, polyphosphates, and the dimer of phosphite called pyrophosphite, was used to determine stability regions for various P species. Calculations were at 25 °C and a pH of 7. As before, the lines of equivalent concentrations for each species were determined as a function of the partial pressure of both $H_2O(g)$ and $H_2(g)$. No counter ion (e.g., Fe^{2+}) was considered in these calculations, as the data was not available for those species. Data for the triphosphate, tetraphosphate, pyrophosphite, and cyclic trimetaphosphate were also not available as a function of temperature, hence all calculations were performed at 25 °C.

Data availability

The data generated in this study are available through the NERC EDS National Geoscience Data Center under https://doi.org/10.5285/09e6ba99-b41a-4ab9-baf4-66c6f5b69fea.

Received: 5 March 2024; Accepted: 28 August 2024;
Published online: 07 September 2024

References

1. Anders, E. & Ebihara, M. Solar-system abundances of the elements. *Geochim. Cosmochim. Acta* **46**, 2363–2380 (1982).
2. Gulick, A. Phosphorus as a factor in the origin of life. *Am. Sci.* **43**, 479–489 (1955).
3. Reinhard, C. T. et al. Evolution of the global phosphorus cycle. *Nature* **541**, 386–389 (2017).
4. Schwartz, A. W. Phosphorus in prebiotic chemistry. *Philos. Trans. R. Soc. B Biol. Sci.* **361**, 1743–1749 (2006).
5. Keefe, A. D. & Miller, S. L. Are polyphosphates or phosphate esters prebiotic reagents? *J. Mol. Evol.* **41**, 693–702 (1995).
6. Pasek, M. A., Gull, M. & Herschy, B. Phosphorylation on the early earth. *Chem. Geol.* **475**, 149–170 (2017).
7. Toner, J. D. & Catling, D. C. A carbonate-rich lake solution to the phosphate problem of the origin of life. *Proc. Natl. Acad. Sci.* **117**, 883–888 (2020).
8. Burcar, B. et al. Darwin's warm little pond: A one-pot reaction for prebiotic phosphorylation and the mobilization of phosphate from minerals in a urea-based solvent. *Angew. Chemie Int. Ed.* **55**, 13249–13253 (2016).
9. Brady, M. P., Tostevin, R. & Tosca, N. J. Marine phosphate availability and the chemical origins of life on Earth. *Nat. Commun.* **13**, 5162 (2022).
10. Pasek, M. A. Rethinking early Earth phosphorus geochemistry. *Proc. Natl. Acad. Sci.* **105**, 853–858 (2008).
11. Herschy, B. et al. Archean phosphorus liberation induced by iron redox geochemistry. *Nat. Commun.* **9**, 1346 (2018).
12. Pasek, M. A., Harnmeijer, J. P., Buick, R., Gull, M. & Atlas, Z. Evidence for reactive reduced phosphorus species in the early Archean ocean. *Proc. Natl. Acad. Sci.* **110**, 10089–10094 (2013).
13. Boden, J. S., Zhong, J., Anderson, R. E. & Stüeken, E. E. Timing the evolution of phosphorus-cycling enzymes through geological time using phylogenomics. *Nat. Commun.* **15**, 3703 (2024).
14. Gull, M., Feng, T., Cruz, H. A., Krishnamurthy, R. & Pasek, M. A. Prebiotic chemistry of phosphite: Mild thermal routes to form condensed-p energy currency molecules leading up to the formation of organophosphorus compounds. *Life* **13**, 920 (2023).
15. Higgs, P. G. & Lehman, N. The RNA World: molecular cooperation at the origins of life. *Nat. Rev. Genet.* **16**, 7–17 (2015).
16. Lohrmann, R. & Orgel, L. E. Prebiotic synthesis: Phosphorylation in aqueous solution. *Science* **161**, 64–66 (1968).
17. Powner, M. W., Gerland, B. & Sutherland, J. D. Synthesis of activated pyrimidine ribonucleotides in prebiotically plausible conditions. *Nature* **459**, 239–242 (2009).
18. Gull, M. et al. Nucleoside phosphorylation by the mineral schreibersite. *Sci. Rep.* **5**, 17198 (2015).
19. Becker, S. et al. Unified prebiotically plausible synthesis of pyrimidine and purine RNA ribonucleotides. *Science (80-.).* **366**, 76–82 (2019).
20. Takabayashi, M., Hirakawa, Y., Kakegawa, T. & Furukawa, Y. Abiotic formation of ribose 5'-phosphate from ribose and apatite with carbonate- and formate-rich solutions. *Geochem. J.* **57**, 134–142 (2023).
21. Hirakawa, Y., Kakegawa, T. & Furukawa, Y. Borate-guided ribose phosphorylation for prebiotic nucleotide synthesis. *Sci. Rep.* **12**, 11828 (2022).
22. Grew, E. S. et al. Boron isotopes in tourmaline from the ca. 3.7–3.8Ga Isua supracrustal belt, Greenland: Sources for boron in Eoarchean continental crust and seawater. *Geochim. Cosmochim. Acta* **163**, 156–177 (2015).
23. Gan, D., Ying, J. & Zhao, Y. Prebiotic chemistry: The role of trimetaphosphate in prebiotic chemical evolution. *Frontiers in Chemistry* **10**, 941228 (2022). vol.
24. Baltscheffsky, M., Schultz, A. & Baltscheffsky, H. H+-proton-pumping inorganic pyrophosphatase: A tightly membrane-bound family. *FEBS Lett.* **452**, 121–127 (1999).
25. Gibard, C. et al. Geochemical sources and availability of amidophosphates on the early earth. *Angew. Chemie Int. Ed.* **58**, 8151–8155 (2019).
26. Krishnamurthy, R., Guntha, S. & Eschenmoser, A. Regioselective alpha-phosphorylation of aldoses in aqueous solution. *Angew. Chem. Int. Ed. Engl.* **39**, 2281–2285 (2000).
27. Kim, H.-J. & Benner, S. A. Prebiotic stereoselective synthesis of purine and noncanonical pyrimidine nucleotide from nucleobases and phosphorylated carbohydrates. *Proc. Natl. Acad. Sci.* **114**, 11315–11320 (2017).
28. Kim, H.-J. & Kim, J. A prebiotic synthesis of canonical pyrimidine and purine ribonucleotides. *Astrobiology* **19**, 669–674 (2019).
29. Sasselov, D. D., Grotzinger, J. P. & Sutherland, J. D. The origin of life as a planetary phenomenon. *Sci. Adv.* **6**, eaax3419 (2023).
30. Pasek, M. A. & Lauretta, D. S. Aqueous corrosion of phosphide minerals from iron meteorites: A highly reactive source of prebiotic phosphorus on the surface of the early earth. *Astrobiology* **5**, 515–535 (2005).
31. Bryant, D. E. & Kee, T. P. Direct evidence for the availability of reactive, water soluble phosphorus on the early Earth. H-Phosphinic acid from the Nantan meteorite. *Chem. Commun*. 2344–2346 https://doi.org/10.1039/B602651F (2006).
32. Ritson, D. J., Mojzsis, S. J. & Sutherland, J. D. Supply of phosphate to early Earth by photogeochemistry after meteoritic weathering. *Nat. Geosci.* **13**, 344–348 (2020).
33. Hess, B. L., Piazolo, S. & Harvey, J. Lightning strikes as a major facilitator of prebiotic phosphorus reduction on early Earth. *Nat. Commun.* **12**, 1535 (2021).
34. de Graaf, R. M. & Schwartz, A. W. Reduction and activation of phosphate on the primitive earth. *Orig. life Evol. Biosph.* **30**, 405–410 (2000).
35. Pasek, M. A. et al. Serpentinization as a route to liberating phosphorus on habitable worlds. *Geochim. Cosmochim. Acta* **336**, 332–340 (2022).

36. van Wazer, J. *Phosphorus and its compounds*. (Interscience Publishers, 1958).
37. Osterberg, R. & Orgel, L. E. Polyphosphate and trimetaphosphate formation under potentially prebiotic conditions. *J. Mol. Evol.* **1**, 241–248 (1972).
38. Yamagata, Y., Watanabe, H., Saitoh, M. & Namba, T. Volcanic production of polyphosphates and its relevance to prebiotic evolution. *Nature* **352**, 516–519 (1991).
39. Pasek, M. A., Kee, T. P., Bryant, D. E., Pavlov, A. A. & Lunine, J. I. Production of potentially prebiotic condensed phosphates by phosphorus redox chemistry. *Angew. Chemie Int. Ed.* **47**, 7918–7920 (2008).
40. de Zwart, I. I., Meade, S. J. & Pratt, A. J. Biomimetic phosphoryl transfer catalysed by iron(II)-mineral precipitates. *Geochim. Cosmochim. Acta* **68**, 4093–4098 (2004).
41. Georgelin, T., Jaber, M., Bazzi, H. & Lambert, J.-F. Formation of activated biomolecules by condensation on mineral surfaces – a comparison of peptide bond formation and phosphate condensation. *Orig. Life Evol. Biosph.* **43**, 429–443 (2013).
42. Paskin, A. et al. Nucleation and crystallization of ferrous phosphate hydrate via an amorphous intermediate. *J. Am. Chem. Soc.* **145**, 15137–15151 (2023).
43. Griffith, E. J., Ponnamperuma, C. & Gabel, N. W. Phosphorus, a key to life on the primitive earth. *Orig. Life* **8**, 71–85 (1977).
44. Frost, R. L., Weier, M. L., Martens, W., Kloprogge, J. T. & Ding, Z. Dehydration of synthetic and natural vivianite. *Thermochim. Acta* **401**, 121–130 (2003).
45. Daou, T. J. et al. Phosphate adsorption properties of magnetite-based nanoparticles. *Chem. Mater.* **19**, 4494–4505 (2007).
46. Wan, B. et al. Iron oxides catalyze the hydrolysis of polyphosphate and precipitation of calcium phosphate minerals. *Geochim. Cosmochim. Acta* **305**, 49–65 (2021).
47. Britvin, S. N. et al. Cyclophosphates, a new class of native phosphorus compounds, and some insights into prebiotic phosphorylation on early Earth. *Geology* **49**, 382–386 (2020).
48. Preiner, M. et al. Serpentinization: Connecting geochemistry, ancient metabolism and industrial hydrogenation. *Life* **8**, 41 (2018).
49. Poulton, S. W. & Canfield, D. E. Ferruginous conditions: A dominant feature of the ocean through earth's history. *Elements* **7**, 107–112 (2011).
50. Burcar, B. et al. A stark contrast to modern earth: Phosphate mineral transformation and nucleoside phosphorylation in an iron- and cyanide-rich early earth scenario. *Angew. Chemie Int. Ed.* **58**, 16981–16987 (2019).
51. Al-Borno, A. & Tomson, M. B. The temperature dependence of the solubility product constant of vivianite. *Geochim. Cosmochim. Acta* **58**, 5373–5378 (1994).
52. Xiong, Y., Guilbaud, R., Peacock, C. L., Krom, M. D. & Poulton, S. W. Phosphorus controls on the formation of vivianite versus green rust under anoxic conditions. *Geochim. Cosmochim. Acta* **351**, 139–151 (2023).
53. Walton, C. R. et al. Evolution of the crustal phosphorus reservoir. *Sci. Adv.* **9**, eade6923 (2023).
54. Früh-Green, G. L., Connolly, J. A. D., Plas, A., Kelley, D. S. & Grobéty, B. Serpentinization of oceanic peridotites: Implications for geochemical cycles and biological activity. *The Subseafloor Biosphere at Mid-Ocean Ridges* 119–136 https://doi.org/10.1029/144GM08 (2004).
55. Sleep, N. H., Meibom, A., Fridriksson, T., Coleman, R. G. & Bird, D. K. H2-rich fluids from serpentinization: Geochemical and biotic implications. *Proc. Natl. Acad. Sci.* **101**, 12818–12823 (2004).
56. McCollom, T. M. Abiotic methane formation during experimental serpentinization of olivine. *Proc. Natl. Acad. Sci.* **113**, 13965–13970 (2016).
57. Holm, N. G., Oze, C., Mousis, O., Waite, J. H. & Guilbert-Lepoutre, A. Serpentinization and the Formation of H2 and CH4 on Celestial Bodies (Planets, Moons, Comets). *Astrobiology* **15**, 587–600 (2015).
58. Mulkidjanian, A. Y., Bychkov, A. Y., Dibrova, D. V., Galperin, M. Y. & Koonin, E. V. Origin of first cells at terrestrial, anoxic geothermal fields. *Proc. Natl. Acad. Sci.* **109**, E821–E830 (2012).
59. Van Kranendonk, M. J. et al. Elements for the origin of life on land: a deep-time perspective from the pilbara craton of Western Australia. *Astrobiology* **21**, 39–59 (2021).
60. Damer, B. & Deamer, D. The hot spring hypothesis for an origin of life. *Astrobiology* **20**, 429–452 (2019).
61. Campbell, K. A. et al. Geyserite in hot-spring siliceous sinter: Window on Earth's hottest terrestrial (paleo)environment and its extreme life. *Earth-Science Rev.* **148**, 44–64 (2015).
62. Westall, F., Brack, A., Fairén, A. G. & Schulte, M. D. Setting the geological scene for the origin of life and continuing open questions about its emergence. *Frontiers in Astronomy and Space Sciences* **9**, 1–1095732 (2023). vol.1095701.
63. Kirkland, D. W., Bradbury, J. P. & Dean, W. E. *The heliothermic lake: a direct method of collecting and storing solar energy (No. 80-807)*. (1980).
64. Ernst, L. et al. Methane formation driven by light and heat prior to the origin of life and beyond. *Nat. Commun.* **14**, 4364 (2023).
65. Watanabe, M., Sato, S. & Saito, H. The mechanism of the hydrolysis of condensed phosphates. II. The mechanism of the degradation of long-chain polyphosphates. *Bull. Chem. Soc. Jpn.* **48**, 896–898 (1975).
66. Watanabe, M., Sato, S. & Saito, H. The mechanism of the hydrolysis of condensed phosphates. III. The mechanism of the hydrolysis of trimeta- and tetrametaphosphates. *Bull. Chem. Soc. Jpn.* **48**, 3593–3597 (1975).
67. Baidya, A. S. & Stüeken, E. E. On-line chloride removal from ion chromatography for trace-level analyses of phosphite and other anions by coupled ion chromatography–inductively coupled plasma mass spectrometry. *Rapid Commun. Mass Spectrom.* **38**, e9665 (2024).
68. Ivey, M. M. & Foster, K. L. Detection of phosphorus oxyanions in synthetic geothermal water using ion chromatography–mass spectrometry techniques. *J. Chromatogr. A* **1098**, 95–103 (2005).
69. Pasek, M. A. Thermodynamics of prebiotic phosphorylation. *Chem. Rev.* **120**, 4690–4706 (2020).
70. Pasek, M. A. & Greenberg, R. Acidification of Europa's subsurface ocean as a consequence of oxidant delivery. *Astrobiology* **12**, 151–159 (2012).

Acknowledgements

The research was funded by the Natural Environment Research Council (NERC) Frontiers Grant -NE/V010824/1 (UK Research and Innovation) to EES. We thank Tomas Lebl, Yuri Andreev, Aamod Desai, Rahul Majee, Pankaj Majhi, Nathan Rochelle-Bates, Alun Barton, and Cristian Savaniu for technical advice and support. Discussions with Barry Herschy, Terrence Kee, and Craig Walton improved the manuscript. We thank Yoshihiro Furukawa and an anonymous reviewer for their comments and suggestions, which have improved the manuscript significantly. For XRD analyses, we acknowledge the Engineering and Physical Science Research Council (EPSRC) Core Equipment Grant (EP/V034138/1).

Author contributions

Conceptualization: E.E.S., A.S.B.. Methodology: A.S.B., E.E.S., M.A.P.. Investigation: A.S.B.. Visualization: A.S.B., M.A.P.. Supervision: E.E.S.. Writing—original draft: A.S.B.. Writing—review & editing: A.S.B., E.E.S., M.A.P.

Competing interests

The authors declare no competing interests.

Additional information

Supplementary information The online version contains supplementary material available at https://doi.org/10.1038/s43247-024-01657-4.

Correspondence and requests for materials should be addressed to Abu Saeed Baidya.

Peer review information *Communications Earth & Environment* thanks Yoshihiro Furukawa and Jonathan Toner for their contribution to the peer review of this work. Primary Handling Editors: Mojtaba Fakhraee and Carolina Ortiz Guerrero. A peer review file is available.